**Full Paper:** The starting point is our previous study of influence of the internal molecular mean field of dipole-dipole interactions on local orientation and phase transitions in polymer liquid crystal (PLC) systems of longitudinal chains.[1, 2] Electric dipoles are created by LC mesogen moieties. The longitudinal PLC is a macromolecule of consecutively copolymerized LC and flexible polymer sequences. We now amplify the model by inclusion of dipole-external electric field interactions. We find that the external fields can seriously modify the local orientational order of the system and affect phase transition parameters dependent on that order. In particular, the external fields induce the formation of disoriented nematic phases with negative values of the second order orientation parameter $\langle P_2 \rangle$ for LC sequences in the longitudinal PLCs while the first order parameter $\langle P_1 \rangle$ is positive. However, some rapid decreases in $\langle P_1 \rangle$ are observed at points of positive-to-negative transitions of $\langle P_2 \rangle$; thus the LC disorientation manifests itself. The limiting case of the monomer liquid crystal (MLC) systems is included also.
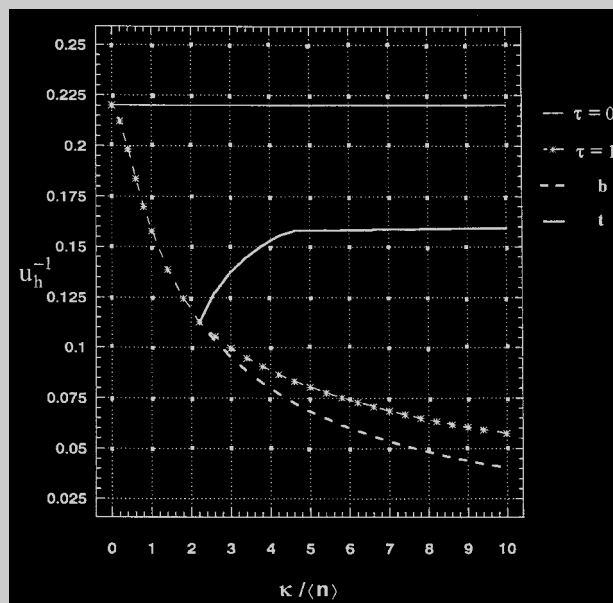
The PLC phase diagram in terms of parameters u_h^{-1} and $\kappa/\langle n \rangle$ (after ref.[2]).

The Influence of External Electric Field on Local Orientations and Phase Transitions in Polymer Liquid Crystals (PLCs)

Witold Brostow,[*,1] *Kazimierz Hibner,*[2] *Janusz Walasek*[1, 2]

[1] Departments of Materials Science and Chemistry, University of North Texas, Denton, TX 76203-5310, USA
[2] Department of Physics, Technical University of Radom, 26-600 Radom, Poland

1. Introduction

The nature of liquid-crystallinity in polymer liquid crystals (PLCs) has been studied using two distinct approaches: lattice and nonlattice. The first method was preferred by Flory who formulated the theory of the athermal PLC systems in his now classic 1956 papers.[3, 4] Flory's model deals with semiflexible longitudinal PLC chain macromolecules. That is, each chain consists of relatively rigid LC and flexible (F) polymer sequences, with both kinds of sequences occurring in the main chain and the LC sequences oriented along the chain backbone.[5–7] Longitudinal PLCs are much different from comb or side chain PLCs – such as investigated experimentally for instance by Springer, Zugenmaier and co-workers.[8–11] They are also different from double PLCs,

with LC sequences both in main and side chains, studied in particular by the University of Halle group[12–16] and also by the Springer group.[17, 18]

In the Flory model the macromolecule is represented by a set of lattice cells. He proposed an ingenious procedure to calculate the system probability.[3, 4] The model requires a small deviation (no larger than $30°$) of LC "hard rods" from a direction of the so-called system symmetry axis; it is the axis of the system cylindrical symmetry. The original theory was subsequently amplified by Flory, his collaborators and students.[19–33] However, an extension of the model to larger angles including $90°$ seems to be rather artificial.

A nonlattice approach was proposed by de Gennes.[34] A PLC system is represented by three semiflexible chains

with mutually perpendicular end-to-end distances. One of them is assumed to be the system symmetry axis; thus two chains perpendicular to this axis are physically equivalent. A chain is not necessarily fully freely-jointed or flexible. The system probability is obtained using conditional optimization of the Helmholtz function functional; one uses the boundary conditions imposed on the chains end-to-end distances. The de Gennes theory was then considered further by Jarry and Monnerie[35] and also by one of us.[36−39]

Both Flory and de Gennes theories are microscopic and use a molecular mean field approach to describe the internal anisotropic orienting interactions. The phases are distinguished with respect to a local orientation, and are characterized by the parameter s which is the average of the second Legendre polynomial P_2 calculated from orientations of LC hard rod particles. s = 0 is for isotropic while s > 0 for nematic phases. Flory and de Gennes theories as well as later theories involving uniaxial orienting interactions[40−43] predict only the transitions from s = 0 to s > 0. Moreover, they do not include in their considerations the presence of an external field, such as electric or magnetic. However, a connection between the external fields and nematic order has been considered using the Landau *phenomenological* formulation of the Helmholtz function as a series in terms of the orientational parameter; see for example Gramsbergen and coworkers.[44]

A nonlattice microscopic theory of PLCs which involves a molecular mean field as well as an external one has been formulated in ref.[1] Presented there is a general thermodynamical description of the system. Specific phase diagrams were obtained for:

i) the mean field theory with s^2 interaction in the Maier and Saupe limit,[45−47] and

ii) the Gaussian limit of the distribution of conformations of F (flexible) sequences within a longitudinal PLC chain.

In ref.[2] the theory of ref.[1] was amplified. Especially, we focused on values of s pertinent to the phase transition lines in PLC phase diagrams.[1, 2] Predictions from the model[2] show that s can be positive as well as negative, in addition to allowing for s = 0. As discussed in ref.,[47] s > 0 means that the system is in the nematic state and has a global nematic symmetry axis, labeled **d**. In this case the probability of orientations of LC hard rod moieties along **d** has a maximal value. For s = 0 the system is isotropic. For s < 0 the probability of the LC direction which is perpendicular to **d** is the highest. In other words, s > 0 represents a system with enhanced direction of the LC units parallel to **d** while s < 0 with enhanced direction perpendicular to **d**. A formal possibility of the last situation in nematic systems was noticed by de Gennes.[47] However, he did not see physical reasons for s < 0 in monomeric liquid crystals (MLCs) which he investigated. Since then some results for MLCs, showing that s > 0 as

well as s < 0 are both possible, have been reported.[48−51] The effect was seen experimentally and theoretically, and stems from a relative flatness of the LC system particles. However, there can be other reasons which can cause this situation:

(1) incorporation of LC particles into a polymer frame in PLCs;

(2) the presence of an external electric field.

For the comb (side chain) PLCs the case (1) was confirmed experimentally in ref.[52−54] and for systems of longitudinal main chain macromolecules in ref.[55−58] The effect was also derived theoretically in ref.[1] and ref.[2] Experimental evidence of the effect (2) in MLCs as well as PLCs exists.[52−54] The main objective of the present article is to investigate the effect (2) for the system of longitudinal PLC chains. Since orientations are created fairly easily in LC systems, the effects we are to trying seize are expect to be significant.

2. General Considerations

This work is a continuation of the theory in[1] and[2], but taking now into account the presence of external electric fields. The probability density function ρ has been calculated in ref.[1] as follows:

$$\rho = C \, \rho_{LC} \, \rho_F \, \delta \tag{1}$$

where ρ_{LC} and ρ_F are, respectively, probabilities of the topologically separated (unconnected) LC and F (flexible polymer) system parts. ρ_{LC} is given by the Gibbs exponential formula[59] whereas ρ_F is obtained using stochastic (random walk) calculations.[1] Constraints pertinent to the topological structure (type of connections) of LC and F sequences in PLC are imposed on ρ by the function δ which is a product of Dirac delta functions.[1] The constant C normalizes ρ to unity.

The Helmholtz function A is calculated using the standard equation:[59]

$$A = U - TS \tag{2}$$

Here U is the system internal energy while S = $-kT\langle \ln \rho \rangle$ is the entropy, and is equal to an average calculated with the distribution ρ; T is the thermodynamic temperature and k is the Boltzmann constant.

The PLC system considered contains N_{ch} longitudinal chains. The number of consecutively copolymerized LC and F sequences per chain is n. The total number of LC sequences in the system is N_h. Thus $N_h = \langle n \rangle N_{ch}$, where $\langle n \rangle$ is the average n value per chain. The general formula for A for such a system given in ref.[1] (see also Equation (A-1) in the Appendix) has been then applied in[1] and[2] to the Maier-Saupe s^2 limit.[44−46] In this approach the LC + LC orienting interactions are replaced by LC + molecular mean field interactions. Our model assumes that each

permanent electric dipole corresponds one-to-one to a LC-vector sequence and is directed along the LC long axis. When, in addition to that molecular field, an external electric field directed along the molecular field appears, the dipole-superposed field interaction energy U takes the form:

$$U = -N_h \left(U_h \langle P_2 \rangle^2/2 + U_{ex} \langle P_1 \rangle \right) \qquad (3)$$

this involves the orientational averages $\langle P_2 \rangle$ and $\langle P_1 \rangle$ of the second and the first Legendre polynomials defined as:

$$P_2 = (3\cos^2\vartheta - 1)/2 \quad \text{and} \quad P_1 = \cos\vartheta \qquad (4)$$

where ϑ is the local deviation angle of the LC-vector direction from a common direction of the molecular and external fields. This direction coincides with the z laboratory axis. The averages $\langle P_2 \rangle = s$ and $\langle P_1 \rangle = s_1$ are calculated over the whole system.

In Equation (3) we also have two positive parameters, U_h and U_{ex}, which respectively pertain to the intensity of interactions between the LC dipoles and the molecular and external fields. In the original articles of Maier and Saupe[44, 45] the potential constant U_h is due to attractive van der Waals forces and is temperature independent. The temperature dependent internal orienting interactions between permanent dipoles are neglected, assumed much weaker than dispersive ones. Experiments made since[60–62] indicate that a contribution from steric repulsion forces may be non-negligible; moreover, U_h does depend on T. Flory and Ronca discussed this problem for PLCs.[20] On this basis, we have used in ref.[31] the following form:

$$U_h = \langle \eta_h \rangle \, \theta \, T^* \qquad (5)$$

where $\langle \eta_h \rangle$ is the average length of LC hard rod sequences in the system. That length is proportional to the LC anisotropy. θ is the concentration of LC sequences in the PLC while T^* is a characteristic temperature which serves as a measure of LC + LC interaction intensity. The measure is normalized to the U_h value taken for unit values of $\langle \eta_h \rangle$ and θ. $U_{ex}P_1$ is the scalar product of the LC permanent dipole moment and the unit vector of an external field. In the following we shall use the reduced parameters $u_h = U_h/kT$ and $u_{ex} = U_{ex}/kT$.

As discussed in the Appendix, the system uniparticle Helmholtz function $\tilde{A}$ is:

$$\begin{aligned}
\tilde{A}/kT &= u_h s(s+1)/2 - \ln f_0 + (1/2\langle n \rangle)(\Lambda_x^2 + \Lambda_y^2 + \Lambda_z^2) \\
&\quad + (3\kappa/2\langle n \rangle)[(\Lambda_x - 1)^2(1 - f_2)/2 + (\Lambda_y - 1)^2(1 - f_2)/2 \\
&\quad + (\Lambda_z - 1)^2(1 - f_2)] \\
&\quad + (3\kappa_1/2\langle n \rangle)(\Lambda_z - 1)^2 f_1^2 + \text{const.}
\end{aligned} \qquad (6)$$

Parameters, Λ_z, Λ_y and Λ_x characterize the deviations from the spherical system symmetry.[1] In our case the

deviations are induced by the presence of both molecular and external fields. Using definitions given by Equation (A3), we obtain for our system:

$$\Lambda_z^2 = [3(\kappa f_2 + \kappa_1 f_1^2) + 1]/(\kappa + 1) \qquad (7)$$

$$\Lambda_x^2 = \Lambda_y^2 = [3(\kappa(1 - f_2)/2 + 1](\kappa + 1) \qquad (8)$$

where κ and κ_1 are:

$$\kappa = \langle \langle \eta_h^2 \rangle_{1\text{int}}/\langle \eta_c \rangle_{1\text{int}} \rangle_1 \qquad (9)$$

$$\kappa_1 = \langle (n-1)\langle \eta_h^2 \rangle_{1\text{int}}/\langle \eta_c \rangle_{1\text{int}} \rangle_1 \qquad (10)$$

As discussed in connection with Equation (5), η_h is the LC sequence length. The end-to-end distance for a F-type sequence is η_c. Averages in (9) and (10) are calculated in two steps: the average with the subscript l int is calculated within a chain, and the average with the subscript l is obtained for the whole system of chains. Parameters κ and κ_1 provide a structural description. This can be shown in a straightforward way for the monodisperse case; then $\langle \eta_h^2 \rangle = \langle \eta_h \rangle^2 = \eta_h^2$ and $\langle \eta_c \rangle = \eta_c$. Consequently, $\kappa_1 = \langle n - 1 \rangle \kappa$ and $\kappa = \eta_h \theta/(1 - \theta)$, where $\theta = \eta_h/(\eta_h + \eta_c)$ is the LC concentration parameter defined in the Flory PLC theory. The uniparticle partition function f_0 and moments f_1 and f_2 are given by:

$$f_0 = \int_{-1}^{1} \exp(u_{ex}z + 3\,u_h s z^2/2)dz \qquad (11)$$

and

$$f_p = \int_{-1}^{1} z^p \exp(u_{ex}z + 3\,u_h s z^2/2)dz/f_0 \qquad (12)$$

where p = 1 or 2.

Equilibria of phases with respect to the orientational order can be recognized by using the equations:

$$\tilde{A}(s_I) = \tilde{A}(s_{II}) = \tilde{A}(s_{III}) = ... \qquad (13)$$

which stem from the chemical potential equivalence in all phases. Phases, indexed by I, II, III, etc., are distinguished with respect to various values of s. Moreover, the Helmholtz function in each phase must exhibit a global minimum at which the derivative $d\tilde{A}/ds$ is equal to zero.

The average s_1 is calculated with the system probability density such as in Equation (A10) in Appendix, with $u(\hat{\eta}_h)$ of the form in (A4), where s is for the system in equilibrium.

3. System Ordering

The present paper is focused on the question: how does the external field modify the PLC properties? Analogous

Table 1. Values of the orientation parameter s and the concentration of the anisotropic phase τ corresponding to dotted points in Figure 1, plus s and τ for κ/⟨n⟩ equal to 0.01 and 0.1. For τ = 0, only the isotropic phase with s = 0 exists; s ≠ 0 is marked by a dash. For τ = 1 the system has one stable, anisotropic phase with s ≠ 0. Isotropic – anisotropic equilibrium exists for τ between 0 and 1. Positive values of s in the relevant cells pertain to the anisotropic phase.

	$u_h^{-1} =$	0.25	0.225	0.2	0.175	0.15	0.125	0.1	0.075	0.05
κ/⟨n⟩ = 0	s =	–	–	0.61	0.72	0.79	0.84	0.88	0.92	0.95
	τ =	0	0	1	1	1	1	1	1	1
κ/⟨n⟩ = 0.01	s =	–	–	0.61	0.72	0.79	0.84	0.88	0.92	0.95
	τ =	0	0	1	1	1	1	1	1	1
κ/⟨n⟩ = 0.1	s =	–	–	0.60	0.72	0.79	0.84	0.88	0.92	0.95
	τ =	0	0	1	1	1	1	1	1	1
κ/⟨n⟩ = 1	s =	–	–	0.41	0.50	0.69	0.80	0.86	0.91	0.94
	τ =	0	0	0.52	0.81	1	1	1	1	1
κ/⟨n⟩ = 2	s =	–	–	0.40	0.46	0.64	0.74	0.83	0.89	0.94
	τ =	0	0	0.34	0.53	0.71	0.93	1	1	1
κ/⟨n⟩ = 3	s =	–	–	0.39	0.44	0.63	−0.21	−0.31	0.88	0.93
	τ =	0	0	0.27	0.42	0.55	0.74	0.99	1	1
κ/⟨n⟩ = 4	s =	–	–	0.39	0.41	−0.08	−0.21	−0.31	0.87	0.93
	τ =	0	0	0.23	0.36	0.47	0.64	0.87	1	1
κ/⟨n⟩ = 5	s =	–	–	0.38	0.39	−0.08	−0.21	−0.31	−0.39	0.93
	τ =	0	0	0.21	0.32	0.42	0.57	0.78	1	1
κ/⟨n⟩ = 6	s =	–	–	0.38	0.35	−0.08	−0.21	−0.31	−0.38	0.92
	τ =	0	0	0.19	0.29	0.38	0.52	0.71	0.99	1
κ/⟨n⟩ = 7	s =	–	–	0.38	0.30	−0.08	−0.21	−0.31	−0.38	0.92
	τ =	0	0	0.17	0.26	0.35	0.48	0.66	0.92	1
κ/⟨n⟩ = 8	s =	–	–	0.38	0.26	−0.08	−0.21	−0.31	−0.38	−0.44
	τ =	0	0	0.16	0.25	0.33	0.45	0.62	0.87	1
κ/⟨n⟩ = 9	s =	–	–	0.38	0.24	−0.08	−0.21	−0.31	−0.38	−0.44
	τ =	0	0	0.15	0.23	0.31	0.42	0.58	0.82	1
κ/⟨n⟩ = 10	s =	–	–	0.37	0.23	−0.08	−0.21	−0.31	−0.38	−0.44
	τ =	0	0	0.14	0.22	0.29	0.4	0.55	0.78	1

properties for the field absence were studied in ref.;[2] that situation corresponds to $U_{ex} = 0$ in Equation (3). Figure 1, based on the results in ref.,[2] shows the system phase diagram in terms of the parameters κ/⟨n⟩ and u_h^{-1}. The lines separate several regions for phases with various s values and the respective phase equilibria are distinguished with respect to s. The phase diagram in Figure 1 is covered by a grid with small square dots. The coordinates of each dot are provided in Table 1. In general, the dot labels a point with s ≠ 0 in an anisotropic phase with the concentration τ, this in addition to s = 0 for the isotropic phase. The parameter τ is equal to $N_{h\,aniso}/(N_{h\,iso} + N_{h\,aniso})$. Here $N_{h\,aniso}$ is the number of LC sequences in the phase with s ≠ 0 and $N_{h\,iso}$ is the analogical number for the phase with s = 0. We clearly have $N_{h\,aniso} + N_{h\,iso} = N_h$. Thus, a map of values of s ≠ 0 and τ is contained in Table 1. For τ = 0 there is no anisotropic phase. For τ = 1 there is no isotropic phase and s > 0 and/or s < 0. The sign of s depends on values of the cell coordinates κ/⟨n⟩ and u_h^{-1}. For 0 < τ < 1 the system is in an isotropic-anisotropic equilibrium.

For more convenient discussion in terms of physical and structural parameters of the PLC, we introduce $u_h^{-1} = kT/T^*θ⟨η_h⟩$ after Equation (5), while $κ = ⟨η_h⟩θ/(1 − θ)$ as noted before. Thus, u_h^{-1} involves the thermal parameters T and T* and also the structural parameters θ and ⟨η_h⟩. An inspection of Figure 1 and Table 1 in these

terms leads to the conclusion that the left upper area of the phase diagram corresponds to the system at high reduced temperatures T/T*; that is high in comparison to the other temperatures in the phase diagram. The LC concentration θ and the LC sequence length ⟨η_h⟩ are relatively low in this area. The right upper area is the part of the phase diagram representing the systems at high temperatures and with high concentration θ of LC sequences. These sequences are long, that is ⟨η_h⟩ values are large. Similarly, the left bottom area corresponds to low T/T* values, low θ and short ⟨η_h⟩. The right bottom part represents low T/T*, high θ and large ⟨η_h⟩ values. The parameter T* is obtained from experimental pressure-volume-temperature (P-V-T) results via an equation of state,[63–67] and depends on details of molecular structure and packing at the molecular level.

Figure 1 and Table 1 have been obtained for a large range of values of the parameters κ/⟨n⟩ and u_h^{-1}. This has been done on purpose, to explore possible kinds of behavior. Not every real system will exhibit all these types of behavior. Thus, systems with s = 0 and s > 0 as well as s < 0 can be found if T, related via κ/⟨n⟩, u_h^{-1} and T* to s, has a physically reasonable value for a given real system.

In Table 1 we have more cells than points marked in Figure 1. Additionally included are κ/⟨n⟩ equal to 0.01 and 0.1. Such small values of κ/⟨n⟩ correspond to PLC
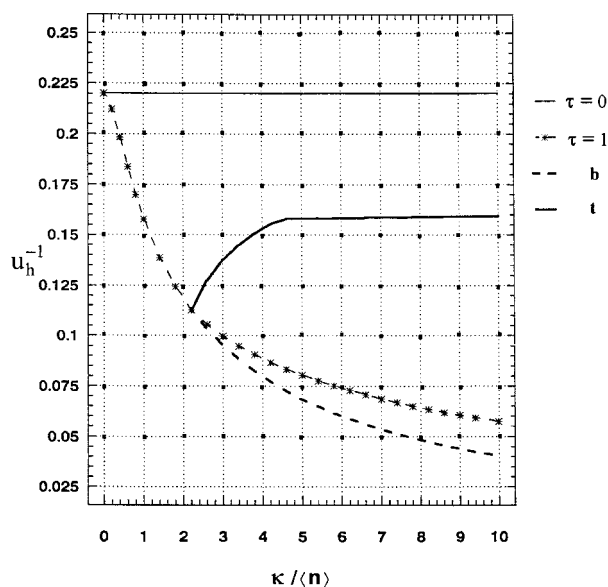
Figure 1. The PLC phase diagram in terms of parameters u_h^{-1} and $\kappa/\langle n \rangle$ (after ref.[2]). u_h^{-1} is proportional to the reduced temperature T/T^* and inversely proportional to $\langle \eta_h \rangle$ and θ. For the monodisperse system for which $\langle \eta_h^2 \rangle = \langle \eta_h \rangle^2$, the parameter is equal to $\langle \eta_h \rangle \theta/(1 - \theta)$. As shown, there are five zones of phase equilibria; there exists the isotropic phase for which $s = 0$. The isotropic-anisotropic equilibria exist in zones for which $s = 0$ and $s > 0$, or $s = 0$ and $s < 0$. Anisotropic phases are in two zones with $s < 0$, and with $s > 0$. Ternary points with $s < 0$, $s = 0$, and $s > 0$ phases in equilibrium are represented by the t line. Binary points with $s < 0$ and $s > 0$ equilibria exist on the b line. Values of the orientation parameter s and concentration τ parameters for the anisotropic phase which pertain to dotted points are listed in Table 1.

Figure 2. The orientation parameter s vs. the intensity of interactions u_{ex} per chain, for $u_h^{-1} = 0.25$. Parameters u_h^{-1} and $\kappa/\langle n \rangle$ are the same as in Figure (1). For u_{ex} the values of s and τ are those listed in Table 1. Modification of s by the external field is illustrated by the plots. The plots are for $\kappa/\langle n \rangle$ equal to 0 (for an MLC), 0.01, 0.1, 1 and 10. The plots for $\kappa/\langle n \rangle$ between 1 and 10 (see again Table 1) have the same character as those for $\kappa/\langle n \rangle$ equal to 1 and 10, and lay between them. The case (a) is for $\langle n \rangle = 10$, case (b) corresponds to $\langle n \rangle = 100$. In both cases we find that for $u_{ex} > 0$ the isotropic phase is an completely unstable, so that $\tau = 1$. A continuous s change near $u_{ex} = 0$, from $s = 0$ to $s > 0$ or $s < 0$ for various $\kappa/\langle n \rangle$, corresponds for a phase transition which is a Curie point.

systems with low LC concentration. In the presence of an external orienting field such a system can exhibit very interesting modifications of phase ordering.

As already noted, the phase diagram in Figure 1 corresponds to $u_{ex} = 0$. It serves us now as a benchmark for the evaluation of effects of switching on an external field, and the consequent modification of internal ordering. The following discussion is based on an analysis of minima of the uniparticle Helmholtz function $\tilde{A}$ in Equation (6) with respect to s and τ, as in Equation (13), taking into account the results in ref.[1, 2]

To begin with, for $u_{ex} > 0$ the parameter $\tau = 1$. This is independent of $\kappa/\langle n \rangle$ and u_h^{-1}. In other words, only the anisotropic phase with $s \neq 0$ is stable. The isotropic phase with $s = 0$ is totally unstable. Under conditions discussed next, the anisotropic phase can split into two phases with $s > 0$ and $s < 0$.

The answer to the question how an increase of u_{ex} is related to s is provided in Figure (2)–(4). Plots labeled (a) are for $\langle n \rangle = 10$ and those labeled (b) for $\langle n \rangle = 100$. Values of u_{ex} per chain are marked on the abscissae and change from 0.01 to 10. To acquire a feeling for the magnitudes involved, the maximum considered value $u_{ex} = 10$
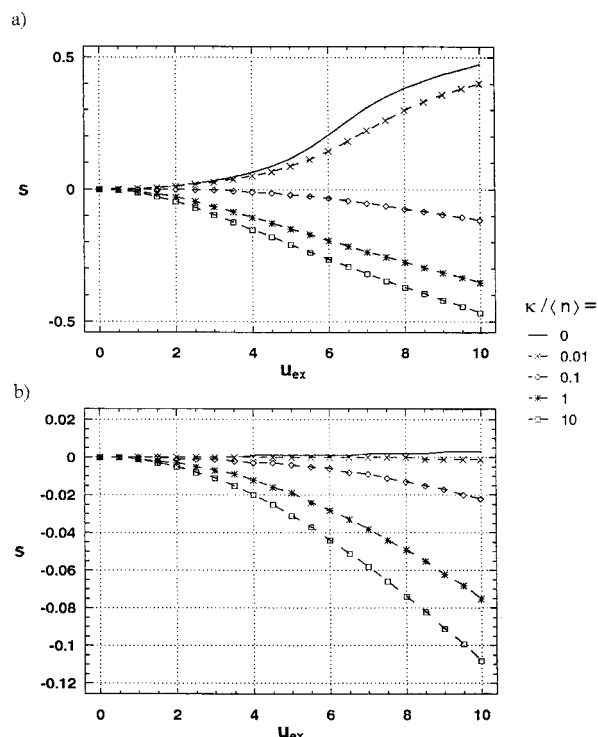
corresponds to the electric field of approximately 10^5 V/cm interacting with a 1 Debye dipole at the temperature of 300 K.

The curves presented are distinguished with respect to $\kappa/\langle n \rangle$ which is equal to 0, 0.01, 0.1, 1 and 10. Curves for $\kappa/\langle n \rangle$ between 1 and 10 are omitted because in these cases changes in the plots are insignificant. The curve for $\kappa/\langle n \rangle = 0$ is related via Equation (6), (7) and (8) to the MLC system of unconnected LC mesogen particles.[1, 2] However, in this case the physical significance of the parameter $\langle n \rangle$ is not exactly the same as in the PLC systems, this due to the connectedness to flexible (F type, naturally unoriented) polymer chain sequences.

For PLCs the system basic element is one chain; u_{ex} values in Figure (2)–(7) are those per single chain. The number of LC sequences per chain $\langle n \rangle$ is a structural parameter. It is related to the number of the chain internal degrees of freedom[1, 2] – and this is why for PLCs we consider separately cases (a) and (b).
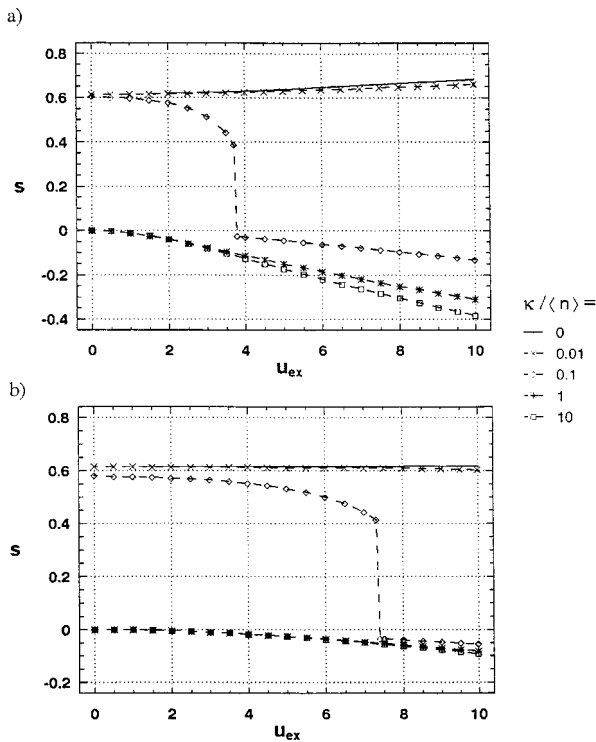
a)

b)

a)

b)

Figure 3. The orientation parameter s vs. the intensity of interactions u_{ex} per chain, for $u_h^{-1} = 0.2$. Parameters and labels are as in Figure (2) and (3). The first order transition from $s > 0$ to $s < 0$ in (a) and (b) cases correspond to $\kappa/\langle n \rangle = 0.1$. Non-first order transitions occurs near $u_{ex} = 0$, for $\kappa/\langle n \rangle$ values equal to 1 and 10.

Figure 4. The orientation parameter s vs. the intensity of interactions u_{ex} per chain, for $u_h^{-1} = 0.1$. In (a) one sees two first order transitions from $s > 0$ to $s < 0$, for $\kappa/\langle n \rangle$ equal to 0.1 and 1. A Curie point transition from $s = 0$ to $s < 0$ occurs $\kappa/\langle n \rangle = 10$. In (b) where $\kappa/\langle n \rangle = 0.1$ the transition vanishes.

For MLCs the system basic element is the LC particle. The uniparticle Helmholtz function $\tilde{A}$ is given by the two first terms of Equation (6), and does not depend on $\langle n \rangle$. In this case the number $\langle n \rangle$ is a formal parameter only which appears in plots pertaining to PLCs and is placed in the same Figure. For an MLC the number $\langle n \rangle$ can be used for rescaling abscissae in Figure (2)–(7) as follows; $u_{ex \, per \, LC} = u_{ex}/\langle n \rangle$. In this case, the plot labeled (b) constitutes the beginning part of the plot labeled (a).

In general, a change of s depends on the variable u_{ex}, and on $\kappa/\langle n \rangle$ as a parameter. In addition and as already noted, we consider cases with two various $\langle n \rangle$ values, as in (a) and (b). The change of s can be either rapid or continuos. According to the Landau classification[68, 69] this means that we have phase transitions of the first or a non-first order; the last ones are also called Curie points. An analysis of Figure (2)–(4) shows for MLCs and low LC concentration PLCs with $\kappa/\langle n \rangle = 0.01$ that an increase of u_{ex} causes an *increase* of s. For $u_h^{-1} = 0.25$ and $\langle n \rangle = 10$ as in Figure (2a), this increase is continuous from s equal to 0 to about 0.5. However, for $\langle n \rangle = 100$ as in Figure (2b), the plot of s vs. u_{ex} for a low LC concentration PLC is a slowly *decreasing* function from zero to a negative value. This means that for a PLC the degree of polymerization $\langle n \rangle$ can change the basic character of the function s vs.
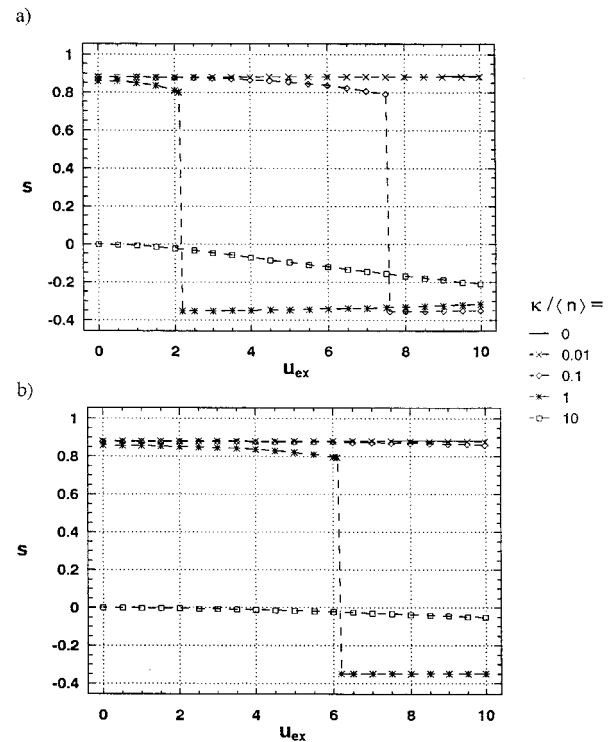
u_{ex}. For PLCs with higher LC concentrations and with $\kappa/\langle n \rangle$ equal to 0.1, 1 and 10, both cases (a) and (b) provide s as a decreasing function of u_{ex}. All plots in Figure (2) change continuously from $s = 0$ to $s \neq 0$. Thus, the respective phase transitions which occur are *not* of the first order.

In the case illustrated in Figure (2), the absence of an external field produces the isotropic phase only. The anisotropic phases with $s > 0$ or $s < 0$ appear when the field is switched on. In Figure (3) and (4) we show how the presence of an external field modifies s in systems in which anisotropic phases already existed before switching on the external field. Figure (3) and (4) are, respectively, for u_h^{-1} equal to 0.2 and 0.1.

Inspection of Figure (3a) shows that s can vary in three distinct ways. For $\kappa/\langle n \rangle$ equal to 0 and 0.01, s is an increasing and a smooth function of u_{ex}. No phase transition from the isotropic to an anisotropic phase is observed. For $\kappa/\langle n \rangle = 0.1$ we observe the first order transition from $s > 0$ to $s < 0$ at a positive u_{ex}, where s changes rapidly. For $\kappa/\langle n \rangle$ equal to 1 and 10, only the Curie point type transition from $s = 0$ to $s < 0$ is observed at $u_{ex} = 0$. The character of the plots in Figure (3b) is generally similar.

In Figure (4a) we observe the appearances of two transitions of the first order. They correspond to two different
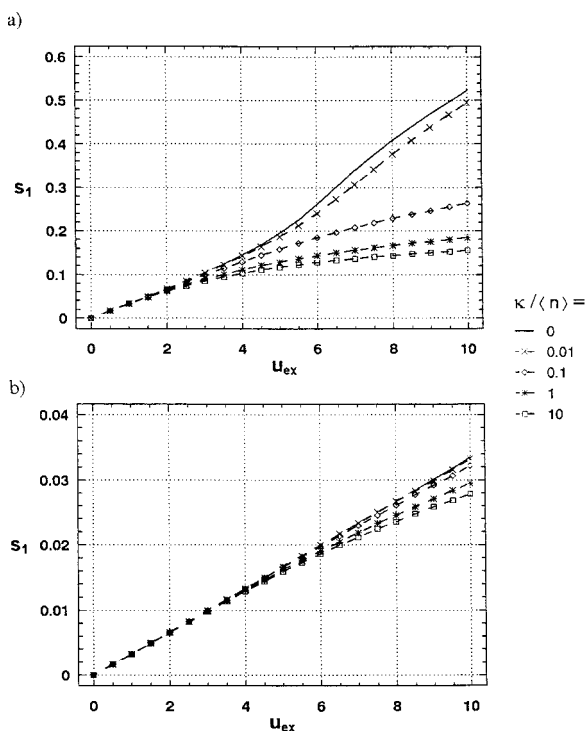
a)

b)

Figure 5. The orientation parameter s_1 vs. the intensity of interactions u_{ex} per chain, for $u_h^{-1} = 0.25$; the $\kappa/\langle n \rangle$ values and phase transition points are as in Figure (2).

a)

b)

Figure 6. The orientation parameter s_1 vs. the intensity of interactions u_{ex} per chain, for $u_h^{-1} = 0.2$; the $\kappa/\langle n \rangle$ values and phase transition points as in Figure (3).

values of u_{ex}, with $\kappa/\langle n \rangle$ equal to 0.1 and 1. In Figure (4 b) this phase transition vanishes for $\kappa/\langle n \rangle = 0.1$, while that for $\kappa/\langle n \rangle = 1$ remains. Changes of s with u_{ex} are representative for values of u_h^{-1} in between 0.22 and 0.05. However, some quantitative differences are predicted. Phase transitions induced by electric field vanish with further decrease of u_h^{-1}. This seems reasonable because of the a very low temperature system in this case.

4. Dipolar Orientations

Averages of odd Legendre polynomials are unvanishable for systems with nematicity disturbed by the presence of external electric field. For characterization of orientational properties in this case at least the first two non-zero averages are required, that is $s \equiv s_2$ and s_1; the former has already been discussed in Section 3. Projection of the LC-dipole **D** on the direction of the external field is called D_E and is equal to $D\cos\vartheta$. The average D_E is $\langle D_E \rangle = D\langle\cos\rangle\vartheta = Ds_1$. It was long ago recognized experimentally that the presence of an elastic part in a PLC system leads to a decrease of $\langle D_E \rangle$ in comparison to that in MLC.[70] For theoretical explanation of this fact de Gennes proposed the *hair pin* model of PLC chain[71] developed further in ref.[72, 73] In this model the *wormlike* chain with permanent electric dipoles connected head-to-tail along the chain contour is subjected to bends, strictly
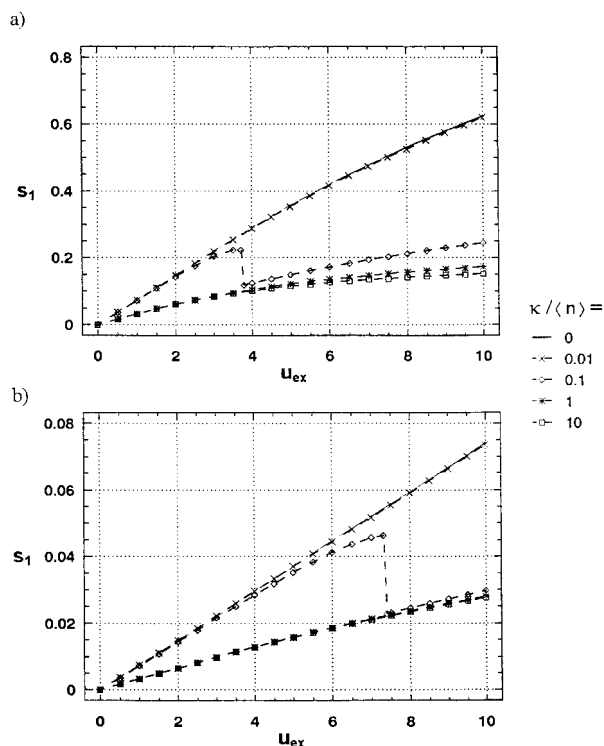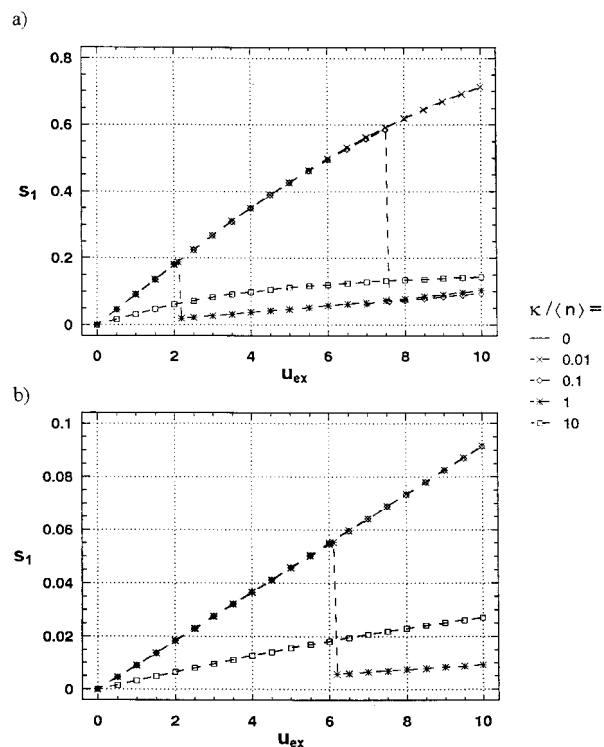
a)

b)

Figure 7. The orientation parameter s_1 vs. the intensity of interactions u_{ex} per chain, for $u_h^{-1} = 0.1$; the $\kappa/\langle n \rangle$ values and phase transition points are as in Figure (4).

speaking to $180°$ about-faces. Thus, only the possibility of parallel and/or antiparallel dipole orientations is allowed. Because of annihilation of some parallel-antiparallel pairs, the resultant $\langle D_E \rangle$ in a PLC is lower than that in a MLC. How much lower it is depends on the number of the about-faces.

We obtain the same effect using the more realistic PLC chain model defined in Section 2. The dipole orientation is a result of *competition* of energetic and entropic mechanisms within the system. There are no preferred dipole orientations, in contrast to those enforced by the hair pin for the parallel-antiparallel dipoles. The results we obtain are illustrated in Figure (5)–(7), as dependencies of s_1 on u_{ex}; note that $\langle D_E \rangle$ is proportional to s_1, and we are using the same set of parameters as in Figure (2)–(4). In general, s_1 is an increasing function of u_{ex}. This tendency is independent of the parameters u_h^{-1} and $\kappa/\langle n \rangle$. However, for some values of u_{ex} a rapid decrease in s_1 is observed. This is illustrated in Figure (6) and (7). We see here a reflection of the system reorganization from a more oriented phase with $s > 0$ to a lower orientation with $s < 0$. The change occurs at the first order transition point discussed in Section 3. A further increase of u_{ex} enhances the orientation and so produces an increase of s_1 but within the less oriented phase.

In Figure (5)–(7) the highest values of s_1 seen in the curves for $\kappa/\langle n \rangle = 0$ it that for the MLC. For PLCs for which $\kappa/\langle n \rangle > 0$, the s_1 values are lower than the analogous ones for the MLC. This difference depends on both parameters used, u_h^{-1} and $\kappa/\langle n \rangle$, and on the variable u_{ex}. In general, the difference between s_1 for a MLC and a PLC is small for low values of u_{ex}. This is especially so for u_h^{-1} equal to 0.25; the case is illustrated in Figure (5a) and (5b). As discussed in Section 3, the anisotropic phase in this case is produced only by the presence of an external electric field. The nematic-like LC + LC interactions are incapable of creation of anisotropic phases because of a high temperature of the system. An increase of $\kappa/\langle n \rangle$ means that the system becomes more dense in LC units. Thus LC orientations are caused primarily by the liquid crystalline mechanism rather than by the external electric field. The LC mechanism takes into account energetic and entropic factors discussed in ref.[1, 2] As a consequence, the s_1 curve is going down with an increase of $\kappa/\langle n \rangle$.

For u_h^{-1} equal to 0.2 and 0.1 the PLC system can produce an anisotropic phase *not necessarily* in the presence of an external field. See again discussion in Section 3, the effect is a consequence of a low temperature of the system. These situations are illustrated in Figure (6) and (7) in terms of s_1 vs. u_{ex} dependence. In Figure (6a) the curves for $\kappa/\langle n \rangle$ equal to 0 (MLC) and 0.01 (poor PLC) are practically the same. For $\kappa/\langle n \rangle = 0.1$ the difference between s_1 for the MLC and the PLC grows with increasing u_{ex}, with the curve slope decreasing rapidly to a nonzero value. We have a reflection of the system ordering

reorganization such as seen in Figure (3a). A further increase of s_1 shows enhanced system organization induced by the external field in the phase with $s < 0$. Curves for $\kappa/\langle n \rangle$ equal to 1 and 10 are very close to each other and are smoothly increasing functions of u_{ex}. The increase is much slower than that for MLCs. Similar situations are seen in Figure (6b) and (7). However, in Figure (7) the s_1 curves for $\kappa/\langle n \rangle$ equal to 0. 0.01, 0.1 and 1 are practically the same but only up to the system reorganization manifested by a rapid decrease of the slope. Stronger differences between the curves appear upon further increase of u_{ex}.

Figure (5)–(7) represent u_h^{-1} in the range defined in Table 1; in (5) we have $u_h^{-1} > 0.23$, and in (6) and (7) $u_h^{-1} < 0.23$. A further decrease in u_h^{-1} leads to the domination of nematic-like forces; consequently, s_1 vanishes.

5. Concluding Remarks

Polymer liquid crystals present a variety of behaviors.[75] The theory presented here predicts $s > 0$ as well as $s < 0$, in addition to $s = 0$. The change of s value is induced by molecular mechanisms: polymerization of LC sequences in a PLC system and/or by an action of an external electric or magnetic field.

The change of the orientation parameter s from a positive to a negative value means that the system undergoes a disorientation of the LC sequences with respect to the nematic axis direction **n**. This effect depends on the physical and structural parameters, such as the system reduced temperature T/T^*, the LC concentration θ, the length of LC sequence $\langle \eta_h \rangle$. Switching on an external electric field can *also* cause the $s > 0$ to $s < 0$ transition. The external field determines the system ordering in each phase. This is reflected in the growth of s_1 with increasing u_{ex}.

Appendix

The general form of the Helmholtz function as given in ref.[1] is:

$$A = -kT \ln \int \ldots \int \exp[-u(\hat{\eta}_h)/kT] p(\hat{\eta}_h, \tilde{\Lambda}^{-1}\hat{r})$$
$$d\hat{\eta}_h d(\tilde{\Lambda}^{-1}\hat{r}) - \langle u(\hat{\eta}_h) \rangle - kT \langle \ln p(\hat{\eta}, \hat{r}) \rangle + U \quad (A1)$$

where U is the system total energy. In our case of orienting interactions we assume that the energy of long-range interactions between a flexible spacer and another element of the system is negligible in comparison with interactions between mesogen LC cores; U is given by Equation (3) in the main text. $\hat{\eta}_h$ labels the set of LC sequence-vectors η_h and $\hat{r}$ labels the set of all chain end-to-end vectors **r**. The symbol $\tilde{\Lambda}^{-1}$ denotes the inverse of the system self-deformation gradient $\tilde{\Lambda}$. This deformation is affine, and is imposed on all vectors of the set $\hat{r}$. The gradient $\tilde{\Lambda}$ has the form of the following diagonal matrix:

$$\tilde{\Lambda} = \begin{bmatrix} \Lambda_x & 0 & 0 \\ 0 & \Lambda_y & 0 \\ 0 & 0 & \Lambda_z \end{bmatrix} \tag{A2}$$

with the components defined by:

$$\Lambda_i^2 = \langle r_i^2 \rangle / \langle r_i^2 \rangle_0; \qquad i = x, y, z \tag{A3}$$

where x, y and z are components of **r** in the laboratory system of Gaussian coordinates. The average with subscript 0 in (A3) pertains to the system which has a spherical symmetry. The average without the index 0 is calculated for the system without the spherical symmetry.[1] Thus, $\tilde{\Lambda}$ is a measure of deviations from the system symmetry, caused by any physical reasons. In our model these deviations stem from the presence of the combined molecular + external field, whereas in the absence of this field the symmetry is assumed to be spherical.

In general, $u(\hat{\eta}_h)$ denotes the internal energy of the LC part of the system. In our case

$$u(\hat{\eta}_h)/kT = -u_{ex} \sum_{j=1}^{N_h} P_{1j} - u_h s \sum_{j=1}^{N_h} P_{2j} \tag{A4}$$

Here the second term containing u_h corresponds to the dipole-molecular field interactions.[44–46] The first term with u_{ex} stems from the dipole-external field interaction. j is the running index over all LC sequences in the system. The orientation parameter s is defined as the average over the whole system, namely

$$s = N_h^{-1} \sum_{j=1}^{N_h} \langle P_{2j} \rangle \tag{A5}$$

The probability $p(\hat{\eta}_h, \hat{r})$ of the state of the set of flexible sequences F in PLC, with $\hat{\eta}_h$ and $\hat{r}$ fixed, is:

$$p(\hat{\eta}_h, \hat{r}) = \prod_{m=1}^{N_{ch}} \left\{ P_{r_c} \left(\sum_{j=1}^{n} \eta_h - \mathbf{r} \right) \right\}_m \tag{A6}$$

where m is the running index over all chains. The function $P_{r_c}(\mathbf{x})$ in (A6), is the integral probability of reaching the vector-distance **r** in r_c random walk steps.[1] It must be pointed out that in our model r_c is the total number of segments per PLC chain. In other words, r_c is the sum of all segments belonging to all flexible spacers of a chain. This ensures large values of r_c. If r_c tends to infinity, the function $P_{r_c}(\mathbf{x})$ becomes Gaussian, and for **x** such as in (A6) it is of the form:[1]

$$P_{r_c} \left(\sum_{j=1}^{n} \eta_{hj} - \mathbf{r} \right) = (3/2 \pi r_c)^{3/2}$$
$$\exp \left[-3 \left(\sum_{j=1}^{n} \eta_{hj} - \mathbf{r} \right) \Big/ 2r_c \right] \tag{A7}$$

where r_c is the number of Kuhn segments. As discussed in,[74] the Gaussian distribution can be used in practice for $r_c > 10$.

The averages in Equation (A1) are:

$$\langle u(\hat{\eta}_h) \rangle = \int \dots \int u(\hat{\eta}_h) P_d(\hat{\eta}_h, \tilde{\Lambda}^{-1}\hat{r}) d\hat{\eta}_h d(\tilde{\Lambda}^{-1}\hat{r}) \tag{A8}$$

and

$$\langle \ln p(\hat{\eta}_h, \hat{r}) \rangle = \int \dots \int P_d(\hat{\eta}_h, \tilde{\Lambda}^{-1}\hat{r}) \ln p(\hat{\eta}_h, \hat{r}) d\hat{\eta}_h d(\tilde{\Lambda}^{-1}\hat{r}) \tag{A9}$$

where P_d is the probability density for the PLC system, and reads:[1]

$$P_d(\hat{\eta}_h, \tilde{\Lambda}^{-1}\hat{r}) = C \exp[-u(\hat{\eta}_h)/kT] p(\hat{\eta}_h, \tilde{\Lambda}^{-1}\hat{r}) \tag{A10}$$

Here C normalizes P_d to unity.

Analogical to those in,[1] calculations of r.h. sides of (A9) and (A10), but for $u(\hat{\eta}_h)$ such as in (A4), followed by calculation of the Helmholtz function A in (A1) for U of the form in Equation (3), give the molar Helmholtz function $\tilde{A} = A/N_h$ displayed as Equation (6) in the main text.

[1] W. Brostow, J. Walasek, *J. Chem. Phys.* **1996**, *105*, 4367.
[2] W. Brostow, K. Hibner, J. Walasek, *J. Chem. Phys.* **1998**, *198*, 6484.
[3] P. J. Flory, *Proc. R. Soc. London, A* **1956**, *234*, 73.
[4] P. J. Flory, *Proc. R. Soc. London, A* **1956**, *234*, 60.
[5] W. Brostow, *Kunststoffe* **1988**, *78*, 411.
[6] W. Brostow, *Polymer* **1990**, *31*, 979.
[7] W. Brostow, in: "*Physical Properties of Polymers Handbook*", J. E. Mark, Ed., American Institute of Physics, Woodbury, NY, 1996, Chap. 33.
[8] F. Gießelmann, P. Zugenmaier, G. Scherowsky, K. Kühnpast, J. Springer, *Makromol. Chem., Rapid Commun.* **1992**, *13*, 489.
[9] K. Kühnpast, J. Springer, G. Scherowsky, F. Gießelmann, P. Zugenmaier, *Liq. Cryst.* **1993**, *14*, 861.
[10] F. T. Niesel, J. Rübner, J. Springer, *Macromol. Chem. Phys.* **1995**, *196*, 4103.
[11] S. Weidner, D. Wolff, J. Springer, *Liq. Cryst.* **1997**, *22*, 193.

[12] U. Rötz, J. Lindau, H. Fischer, F. Kuschel, *Polym. Bull. (Berlin)* **1992**, *27,* 481.

[13] A. Böhme, J. Lindau, U. Rötz, F. Hoffmann, H. Fischer, S. Diele, F. Kuschel, *Makromol Chem.* **1992**, *193,* 2581.

[14] A. Böhme, E. Novotna, H. Kresse, F. Kuschel, J. Lindau, *Makromol. Chem.* **1993**, *194,* 3341.

[15] U. Rötz, J. Lindau, H. Fischer, F. Kuschel, *Mol. Cryst. Liq. Cryst.* **1993**, *225,* 167.

[16] U. Emmerling, S. Diele, H. Schmalfuß, J. Werner, H. Kresse, J. Lindau, *Macromol. Chem. Phys.* **1998**, *199,* 1529.

[17] G. Galli, E. Chiellini, M. Laus, D. Ferri, D. Wolff, J. Springer, *Macromolecules* **1997**, *30,* 3417.

[18] G. Galli, E. Chiellini, O. Francescangeli, D. Ferri, D. Wolff, J. Springer, M. Laus, S. Angeloni, *Macromol. Symp.* **1997**, *121,* 235.

[19] P. J. Flory, G. Ronca, *Mol. Cryst. Liq. Cryst.* **1979**, *54,* 289.

[20] P. J. Flory, G. Ronca, *Mol. Cryst. Liq. Cryst.* **1979**, *54,* 311.

[21] P. J. Flory, A. Abe, *Macromolecules* **1978**, *11,* 1119.

[22] A. Abe, P. J. Flory, *Macromolecules* **1978**, *11,* 1122.

[23] P. J. Flory, R. S. Frost, *Macromolecules* **1978**, *11,* 1126.

[24] R. S. Frost, P. J. Flory, *Macromolecules* **1978**, *11,* 1134.

[25] P. J. Flory, *Macromolecules* **1978**, *11,* 1138.

[26] P. J. Flory, *Macromolecules* **1978**, *11,* 1141.

[27] R. R. Matheson, P. J. Flory, *Macromolecules* **1981**, *14,* 954.

[28] P. J. Flory, P. A. Irvine, *J. Chem. Soc., Faraday Trans.* **1984**, *80,* 1807.

[29] P. J. Flory, R. R. Matheson Jr., *J. Chem. Phys.* **1985**, *88,* 6006.

[30] R. R. Matheson Jr., *Macromolecules* **1986**, *19,* 1286.

[31] D. A. Jonah, W. Brostow, M. Hess, *Macromolecules* **1993**, *26,* 76.

[32] S. Blonski, W. Brostow, D. A. Jonah, M. Hess, *Macromolecules* **1993**, *26,* 84.

[33] W. Brostow, J. Walasek, *Macromolecules* **1994**, *27,* 2923.

[34] P. G. de Gennes, *C. R. Hebd. Seances Acad. Sci. B* **1975**, *281,* 101.

[35] J. P. Jarry, L. Monnerie, *J. Polym. Sci., Polym. Phys. Ed.* **1978**, *16,* 443.

[36] J. Walasek, *J. Polym. Sci., Polym. Phys. Ed.* **1988**, *26,* 1907.

[37] J. Walasek, *J. Polym. Sci., Polym. Phys. Ed.* **1990**, *28,* 1075.

[38] J. Walasek, *J. Polym. Sci., Polym. Phys. Ed.* **1990**, *28,* 2473.

[39] J. Walasek, *J. Polymer Sci., Phys. Ed.* **1992**, *30,* 401.

[40] D. J. Photinios, E. T. Samulski, J. Toriumi, *J. Phys. Chem.* **1990**, *94,* 4688.

[41] D. J. Photinios, E. T. Samulski, J. Toriumi, *J. Phys. Chem.* **1990**, *94,* 4694.

[42] D. J. Photinios, E. T. Samulski, J. Toriumi, *J. Chem. Phys.* **1991**, *95,* 2758.

[43] D. J. Photinios, E. T. Samulski, J. Toriumi, *Mol. Cryst. Liq. Cryst.* **1991**, *204,* 161.

[44] E. F. Gramsbergen, L. Longa, W. H. deJeu, *Phys. Reports* **1986**, *135,* 195.

[45] W. Maier, A. Saupe, *Z. Naturforsch.* **1959**, *A14,* 882.

[46] W. Maier, A. Saupe, *Z. Naturforsch.* **1960**, *A15,* 287.

[47] P. G. de Gennes, "*The Physics of Liquid Crystals*", Clarendon Press, Oxford 1974.

[48] M. J. Freiser, *Phys. Rev. Lett.* **1970**, *19,* 1041.

[49] L. J. Yu, A. Saupe, *Phys. Rev. Lett.* **1980**, *12,* 1000.

[50] L. J. Yu, A. Saupe, *J. Am. Chem. Soc.* **1980**, *102,* 4879.

[51] K. Praefcke, B. Kohne, B. Gundogan, D. Singer, D. Demus, S. Diele, G. Peltzl, M. Bakowsky, *Mol. Cryst. Liq. Cryst.* **1991**, *198,* 393.

[52] F. Hessel, H. Finkelmann, *Polym. Bull. (Berlin)* **1986**, *15,* 449.

[53] F. Hessel, R. P. Herr, H. Finkelmann, *Makromol. Chem.* **1987**, *188,* 1597.

[54] M. Ballauff, *Angew. Chem.* **1988**, *5,* 775.

[55] C. Viney, G. R. Mitchell, A. H. Windle, *Polym. Commun.* **1983**, *24,* 145.

[56] A. H. Windle, C. Viney, R. Golombok, A. M. Donald, G. R. Mitchell, *Faraday Discuss. Chem. Soc.* **1985**, *79,* 55.

[57] A. M. Donald, C. Viney, A. H. Windle, *Phil. Mag.* B **1985**, *52,* 925.

[58] T. De'Neve, M. Kleman, P. Navard, *J. Phys. II France* **1992**, *2,* 187.

[59] E. A. Guggenheim, "*Thermodynamics*", 5th Ed., North-Holland, Amsterdam 1967.

[60] S. Chandrasekhar, "*Liquid Crystals*", Cambridge Univ. Press, 1977.

[61] P. G. de Gennes, J. Prost, "*The Physics of Liquid Crystals*", 2nd Ed., Clarendon Press, Oxford 1993.

[62] M. Ballauff, in: "*Materials Science and Technology*", Vol. 12, R. W. Cahn, P. Haasen, J. Kramer, Eds., VCH Publishers, Weinheim-New York-Basel-Cambridge-Tokyo, 1993.

[63] P. J. Flory, *J. Am. Chem. Soc.* **1956**, *87,* 1833.

[64] P. J. Flory, *Disc. Faraday Soc.* **1970**, *49,* 7.

[65] B. Hartmann, *Proc. Can. High Polym. Forum* **1983**, *22,* 20.

[66] B. Hartmann, M. A. Haque, *J. Appl. Phys.* **1985**, *58,* 283.

[67] B. Hartmann, M. A. Haque, *J. Appl. Polym. Sci.* **1985**, *30,* 1953.

[68] L. Landau, E. Lifshitz, "*Statistical Physics*", Addison-Wesley, Reading, MA, 1958.

[69] L. Landau, "*Collected Papers*", D. ter Haar, Ed., Gordon and Breach, New York 1956.

[70] V. N. Tsvetkov, V. E. Erskin, S. Y. Frenkel, "*Struktura Makromolekul v Roztworah*", Nauka, Moscow 1964.

[71] P. G. de Gennes, in: "*Polymer Liquid Crystals*", A. Ciferri, W. R. Krigbaum, B. Maier, Eds., Academic Press, New York 1982.

[72] M. Gunn, M. Warner, *Phys. Rev. Lett.* **1987**, *58,* 393.

[73] B. Heldman, M. Warner, *Macromolecules* **1998**, *31,* 3519.

[74] P. J. Flory, "*Statistical Mechanics of Chain Molecules*", Wiley-Interscience, New York 1969.

[75] W. Brostow, Ed., "*Mechanical and Thermodynamical Properties of Polymer Liquid Crystals*", Chapman & Hall, London 1998.